Gas-Phase Transuranium Organometallic Chemistry: Reactions of Np^+, Pu^+, NpO^+, and PuO^+ with Alkenes

John K. Gibson

Contribution from the Chemical and Analytical Sciences Division, Oak Ridge National Laboratory, Oak Ridge, Tennessee 37831-6375

Received September 10, 1997

Abstract: The study of gas-phase organometallic chemistry has been extended to the first two transuranium elements, Np and Pu. Product abundances were determined for reactions of the alkenes, L = ethene, *cis*-2-butene, cyclohexene, and 1,5-cyclooctadiene (COD), with Np^+, NpO^+, Pu^+, and PuO^+, and comparison was made with results for Th^+, U^+, ThO^+, and UO^+. A key finding was that U^+ and Np^+ were comparably effective at dehydrogenation of ethene and 2-butene whereas Pu^+ was less effective, consistent with a conventional mechanism of dehydrogenation via oxidative insertion of a prepared "divalent" M^+ into a C−H bond (i.e., C−An^+−H, where An = actinide). The reduced reactivity of Pu^+ indicates that its 5f electrons do not participate in C−H bond activation. The smaller discrepancy between U^+ and Np^+ compared with Pu^+ which was found using cyclohexene and COD as reactants can be attributed to their greater polarizabilities and allylic C−H bonds. The linear alkenes were essentially inert toward all of the AnO^+, but cyclohexene was dehydrogenated by UO^+ and ThO^+ and COD was dehydrogenated by all four AnO^+. With COD, single H_2 loss was dominant for NpO^+ and PuO^+, while double dehydrogenation was the primary pathway for UO^+ and ThO^+; it appears that C−H activation occurred by different mechanisms and that the 5f electrons of UO^+ may facilitate C−H activation whereas the 5f electrons of NpO^+ and PuO^+ are inert. The relatively high reactivity of ThO^+ accords with the classification of Th as a pseudo-d-block transition element.

Introduction

Gas-phase organometallic chemistry is widely applied to elucidating fundamental interactions between metal ions, M^+, and organic substrates in the absence of solvation and competing reaction pathways.[1] Of particular interest is the activation of hydrocarbons accompanied by complexation of resulting fragment ligands to the metal ion: $M^+ + L \rightarrow M^+{-}L^* + C_{n'}H_{m'}$. Mechanisms of C−H and C−C activation and the bonding in the resulting complex ions have been probed for a variety of substrates and M^+, with particular emphasis on first-row transition metals.[2]

Variations in condensed-phase organometallic chemistry among the lanthanide (Ln) elements are minor, reflecting the inert character of the localized 4f orbitals. Organolanthanide chemistry is dominated by ionic Ln^{III} complexes in which three valence 5d/6s electrons bond with an electrophile such as cyclopentadienyl, C_5H_5 (Cp) (e.g., $Ln^{3+}Cp^-_3$).[3] In contrast, *gas-phase* Ln^+ ions require widely disparate energies to excite a nonreactive 4f electron to a valence 5d orbital—from zero for Ce^+ (ground state = $4f^15d^2$) to 394 kJ mol^{-1} for Eu^+ [4]—and widely discrepant chemistries are manifested. Schilling and Beauchamp[5] initiated the study of gas-phase lanthanide organometallic chemistry and interpreted their results to indicate that the 4f orbitals of Ln^+ were ineffective in C−H (or C−C) activation; evidently, excitation of ground Ln^+ to a "divalent" state with two non-f valence electrons (e.g., $4f^{n-2}5d^16s^1$) was required for oxidative insertion of Ln^+ into a C−H bond. The terminology "divalent" here designates a M^+ which has been "prepared" for formation of two covalent bonds. Subsequent studies[6−8] have confirmed the validity of this model, which is illustrated in Scheme 1 for dehydrogenation of 1-butene. The consistency of results with Ln^+ [8] demonstrated the value of a technique which involves reacting nascent laser-ablated ions with a gas and determining abundances of product ions within ~100 μs. This approach, referred to as "laser ablation with prompt reaction and detection" (LA/PRD) revealed compara-

Scheme 1

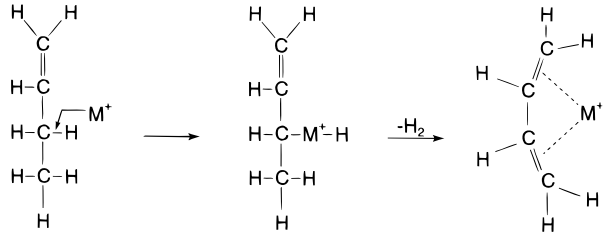

(1) (a) Eller, K.; Schwarz, H. *Chem. Rev.* **1991**, *91*, 1121−1177. (b) Armentrout, P. B. In *Gas-Phase Inorganic Chemistry*; Russell, D. H., Ed.; Plenum Press: New York, 1989; pp 1−42. (c) Freiser, B. S. *Acc. Chem. Res.* **1994**, *27*, 353−360. (d) Armentrout, P. B.; Baer, T. *J. Phys. Chem.* **1996**, *100*, 2866−2877. (e) Bowers, M. T.; Marshall, A. G.; McLafferty, F. W. *J. Phys. Chem.* **1996**, *100*, 2897−2910.

(2) (a) Freiser, B. S. *J. Mass Spectrom.* **1996**, *31*, 703−715. (b) Carpenter, C. J.; van Koppen, P. A. M.; Bowers, M. T. *J. Am. Chem. Soc.* **1995**, *117*, 976−985.

(3) Schumann, H.; Genthe, W. In *Handbook on the Physics and Chemistry of Rare Earths*; Gschneidner, K. A., Jr.; Eyring, L., Eds.; Elsevier: New York, 1984; Vol. 7, pp 445−571.

(4) Martin, W. C.; Zalubas, R.; Hagan, L. *Atomic Energy Levels − The Rare-Earth Elements*; National Bureau of Standards: Washington, DC, 1978.

(5) Schilling, J. B.; Beauchamp, J. L. *J. Am. Chem. Soc.* **1988**, *110*, 15−24.

(6) Yin, W. W.; Marshall, A. G.; Marcalo, J.; Pires de Matos, A. *J. Am. Chem. Soc.* **1994**, *116*, 8666−8672.

(7) Cornehl, H. H.; Heinemann, C.; Schroder, D.; Schwarz, H. *Organometallics* **1995**, *14*, 992−999.

(8) Gibson, J. K. *J. Phys. Chem.* **1996**, *100*, 15688−15694.

S0002-7863(97)03182-X CCC: $15.00
Published on Web 03/05/1998

Table 1. Ground-State Configurations and Excitation Energies for An^+ [a]

	ground state	lowest "divalent" state[b]	ΔE (kJ mol^{-1})
Th^+	$5f^5 6d^2 7s^1$	ground	0
U^+	$5f^5 7s^2$	$5f^5 6d^1 7s^1$	3
Np^+	$5f^5 6d^1 7s^1$	ground	0
Pu^+	$5f^5 7s^1$	$5f^5 6d^1 7s^1$	104

[a] Reference 18. [b] Lowest energy configuration with ≥2 unpaired non-f electrons; ΔE is for the lowest *J*-term; within the present context, the filled 7s subshell of ground U^+ may also be considered as "divalent."

tive intrinsic Ln^+ reactivities despite potential effects of internal and translational energies.[9]

Actinide (An) organometallic chemistry has concentrated mainly on Th and U, which are abundant and present relatively minor radiological hazards.[10,11] Whereas the early actinides somewhat resemble d-block transition elements in their organometallic chemistry, increasingly lanthanide-like behavior is exhibited in progressing across the series and $AnCp_3$ are among the few organometallics isolated for the transplutonium actinides. The transition in the actinide series from quasi-d-block to lanthanide-like chemistry occurs between Th and Am; Pa, U, Np and Pu exhibit several oxidation states and variable involvement of the 5f orbitals in bonding.[12] Early work on the gas-phase chemistry of U^+ was carried out by Armentrout et al.,[13,14] and recent studies of hydrocarbon activation by U^+ [15] and Th^+ [16] indicated reactivities consistent with the oxidative insertion mechanism established for Ln^+ (Scheme 1); consistent results were obtained by LA/PRD.[17] Both Th^+ and U^+ possess "divalent" configurations with two non-5f valence electrons in (or near) their ground states (Table 1)—this precluded interpreting their reactivities in the context of the role of the 5f orbitals. Whereas Np^+ also has a "divalent" ground-state configuration, the promotion energy of Pu^+ is sufficiently large that reduced reactivity should be manifested *unless* the 5f electrons of Pu^+ can directly participate in hydrocarbon activation. The role of 5f electrons in gas-phase organoactinide chemistry was probed here by comparing reactivities of Th^+, U^+, Np^+, and Pu^+.

A recent study of reactions of LnO^+ with butadiene[19] revealed a remarkable variability in hydrocarbon activation efficiencies which correlated with LnO^+ polarizabilities as estimated by the ionization energies, IE[LnO]. It was also recently reported[20] that ThO^+ and UO^+ are efficient at dehydrogenating cyclohexadiene, while CeO^+ is nearly inert, consistent with LA/PRD results.[17] The greater reactivity of ThO^+ compared with CeO^+ can be attributed to the larger IE of ThO and the presence of a chemically active 6d/7s (rather than 5f) radical electron at the metal center of ThO^+.[20] The reactivity of UO^+ might be attributed to oxidative insertion of the unsaturated metal center into a C−H bond, implying participation of 5f electrons.[19] A second goal of the present study was to assess the reactivities of transuranium AnO^+ for comparison with lighter congeners.

Experimental Section

The experimental methods used to apply LA/PRD to assessing the gas-phase reactivities of lanthanide[8] and actinide[17] ions with organic substrates have been described previously, and only a summary of key features of the experiment are included here. These studies were performed in the Transuranium Research Laboratory at ORNL which is designed to allow experimental investigation of the elements Np through Fm. The LA/PRD approach was developed due to its simplicity compared with techniques such as FTICR-MS and the relative ease of adaptation to transuranium studies. A recent modification to the laser ablation mass spectrometer employed in earlier studies was its installation into a glovebox designed to contain highly radioactive transuranium materials. The beam of the ablating XeCl excimer laser (λ = 308 nm) entered the glovebox through a silica window and was focused to a ∼0.5 mm^2 spot on a solid target. The energy incident on the target was ∼2 mJ pulse^{-1}, giving an average irrradiance of ∼10^7 W cm^{-2} (pulse duration, 15 ns). The reactant gas (L) was bled through a leak valve into a ∼1 mm i.d. tube and injected into the path of the ablated ions, ∼1 cm from the target surface. The local reactant pressure encountered by ablated ions was undetermined but was maintained approximately constant. The base pressure in the mass spectrometer flight tube of ∼10^{-7} mbar increased to ∼10^{-6} mbar upon admitting the gas, and the reactant pressure near the target must have been significantly greater (e.g., ≳10^{-4} mbar). Ions resulting from condensation of multiple ligands onto a M^+—which occurs at comparable pressures in other techniques—were minor, presumably reflecting the short flight path and reaction time (which was insufficient for significant radiative cooling of initial products). After traveling ∼3 cm through the reactant gas perpendicular to the flight tube axis, positive ions—unreacted M^+ and MO_n^+ and product M^+−L* and MO^+−L*—were injected into the reflectron time-of-flight mass spectrometer by a +200 V pulse on an ion repeller plate. This ion extraction configuration sampled a ∼6 mm diameter transverse cylindrical cross section of the ablation plume. By varying the time delay, t_d, between the laser pulse and ion injection it was possible to sample ions with different velocities (kinetic energies). The standard value of t_d used in the present study was ∼35 μs which typically provided optimal sensitivity to most products. The standard t_d corresponds to an ablated ion velocity of {(∼3 cm)/(∼35 μs)} ≈ 1 km s^{-1} and an ion kinetic energy ($KE_I = \{1/2\} m_I v_I^2$) of ∼120 kJ mol^{-1} for an An^+ (or AnO^+) of mass ∼240 Da. The center-of-mass energy (KE_{CM}) imparted in the collision of these projectile ions with a quasi-stationary reactant molecule, L, is approximated by $KE_{CM} \approx KE_I\{m_L/(m_I + m_L)\}$. The estimated KE_{CM} (in kJ mol^{-1}) for the present experiments are ∼13 for C_2H_4, ∼23 for C_4H_8, ∼31 for C_6H_{10}, and ∼37 for C_8H_{12}. *All of the reported reactions involved hyperthermal ions.*

The ablation targets were prepared by mixing powders of metal dioxides with copper and compressing the aggregate into a 3-mm diameter pellet using a small manual pellet press in a transuranic glovebox. The following constituents were commercial products: 99.999% Cu°; 99.99% TiO_2; 99.9% CeO_2; 99.9% ThO_2 (natural Th = 100% ^{232}Th); and 99.8% UO_2 (depleted U = 99.55% ^{238}U). The transuranium materials were archival ORNL samples: $^{237}NpO_2$ (>99.9% ^{237}Np) and $^{242}PuO_2$ (99.7% ^{242}Pu). The scarce ^{242}Pu isotope (half-life ($t_{1/2}$) = 4 × 10^5 y) was selected due to its low specific radioactivity compared with more common isotopes such as ^{239}Pu ($t_{1/2}$ = 2 × 10^4 y) and ^{240}Pu ($t_{1/2}$ = 7000 y); each decays primarily by α-emission. An additional advantage of ^{242}Pu was its greater mass separation from ^{237}Np and ^{238}U. The three targets are designated as follows with the aggregate compositions expressed as molar percent of metal content:

(9) (a) Sunderlin, L. S.; Armentrout, P. B. *J. Am. Chem. Soc.* **1989**, *111*, 3845−3855. (b) Gidden, J.; van Koppen, P. A. M.; Bowers, M. T. *J. Am. Chem. Soc.* **1997**, *119*, 3935−3941.

(10) Marks, T. J.; Streitwieser, A., Jr. In *The Chemistry of the Actinide Elements*, 2nd ed.; Katz, J. J., Seaborg, G. T., Morss, L. R., Eds.; Chapman and Hall: New York, 1986; Vol. 2, pp 1547−1587.

(11) Marks, T. J. In *The Chemistry of the Actinide Elements*, 2nd ed.; Katz, J. J., Seaborg, G. T., Morss, L. R., Eds.; Chapman and Hall: New York, 1986; Vol. 2, 1588−1628.

(12) Katz, J. J.; Morss, L. R.; Seaborg, G. T. In *The Chemistry of the Actinide Elements*, 2nd ed.; Katz, J. J., Seaborg, G. T., Morss, L. R., Eds.; Chapman and Hall: New York, 1986; Vol. 2, pp 1121−1195.

(13) Armentrout, P. B.; Hodges, R. V.; Beauchamp, J. L. *J. Am. Chem. Soc.* **1977**, *99*, 3162−3163.

(14) Armentrout, P. B.; Hodges, R. V.; Beauchamp, J. L. *J. Chem. Phys.* **1977**, *66*, 4683−4688.

(15) Heinemann, C.; Cornehl, H. H.; Schwarz, H. *J. Organomet. Chem.* **1995**, *501*, 201−209.

(16) Marcalo, J.; Leal J. P.; Pires de Matos, A. *Int. J. Mass Spectrom. Ion Processes* **1996**, *157/158*, 265−274.

(17) Gibson, J. K. *Organometallics* **1997**, *16*, 4214−4222.

(18) Fred, M. S.; Blaise, J. In *The Chemistry of the Actinide Elements*, 2nd ed.; Katz, J. J., Seaborg, G. T., Morss, L. R., Eds.; Chapman and Hall: New York, 1986; Vol. 2, pp 1196−1277.

(19) Cornehl, H. H.; Wesendrup, R.; Harvey, J. N.; Schwarz, H. *J. Chem. Soc., Perkin Trans. 2* **1997**, 2283−2291.

(20) Cornehl, H. H.; Wesendrup, R.; Diefenbach, M.; Schwarz, H. *Chem. Eur. J.* **1997**, *3*, 1083−1090.

Table 2. Atom and Oxide Ionization Energies (IE) and Monoxide Dissociation Energies ($D_0°$)[a]

M	IE[M]	IE[MO]	IE[MO_2]	$D_0°$[MO]	$D_0°$[MO^+][b]
Th	588(11)	589(10)	840(20)	873(10)	870(30)
U	598(1)	550(20)	530(50)	755(10)	800(30)
Np	605(1)	550(10)	480(50)	736(50)	770(60)
Pu	585(2)	560(50)	910(50)	680(60)	710(110)

[a] All values are kJ mol^{-1}; uncertainties are indicated in parentheses. All IE are from ref 22; $D_0°$[MO] are from ref 21, except $D_0°$[PuO] is from ref 23. [b] $D[MO^+] = D[MO] - IE[MO] + IE[M]$.

U−Pu = 3.9% U + 3.0% Pu + 93% Cu; **Np−Pu** = 1.2% Np + 1.5% Pu + 97% Cu; and **Ce−Th−(Pu)** = 1.8% Ti + 1.8% Ce + 5.0% Th + 91% Cu (+ trace Pu). Although the intended role of this last target was to produce Ti^+, Ce^+, and Th^+, negligible Ti^+ was generated, presumably reflecting the relatively high ionization energy, IE[Ti] = 658 kJ mol^{-1};[21] the substantial amounts of Pu^+ from this target due to Pu contamination reflected the low IE[Pu]. The **U−Pu** and **Np−Pu** targets incorporated ∼2−6 mg of the transuranic oxides.

Four alkene reactants were employed on the basis of their discrepant propensities toward dehydrogenation, which increase in the order: ethene < *cis*-2-butene < cyclohexene < 1,5-cyclooctadiene (COD); the last three are also susceptible to C−C activation and cracking although dehydrogenation has proved the most reliable indicator of comparative Ln^+, An^+, and AnO^+ reactivities using LA/PRD and is emphasized here. The alkenes were commercial products with the following purities: 99.99% ethene, C_2H_4; ≥95% *cis*-2-butene, C_4H_8; 99% cyclohexene, *c*−C_8H_{10}; 99% COD, 1,5-*c*−C_8H_{12}. The liquid reagents were subjected to at least two freeze−evacuate−thaw cycles prior to use, and all gases were introduced into the reaction region as described above.

Results and Discussion

The reported complex ion abundances, $A[M^+-L^*]$, are referenced to the naked M^+ (or MO^+) ion intensity (peak height), $I[M^+]$, as follows: $A[M^+-L^*] = \{I[M^+-L^*]/I[M^+]\} \times 100$; $A[MO^+-L^*] = \{I[MO^+-L^*]/I[MO^+]\} \times 100$. Multiplication of the intensity ratio by 100 gives product yields as a percentage of the unreacted parent ion. Uncertainties in the reported abundances (generally ∼10%) are specified in the Tables. The mass resolution was sufficient to differentiate $M^+-C_nH_m$ from $M^+-C_nH_{m+2}$.

Substantial amounts of AnO^+ and UO_2^+ were ablated from the targets. The relative abundances of $An^+/AnO^+/AnO_2^+$ co-ablated from a target apparently reflected the oxide dissociation energies and ionization energies (Table 2). The qualitative ordering of oxide ion abundances was as follows: $UO^+ > ThO^+ > NpO^+ > PuO^+$; representative monoxide ion intensities are indicated in the tables and figures. The propensity to produce AnO^+ in the ablation plume can be considered in the context of the monoxide ionization energies and dissociation energies: low IE[AnO] enhances ionization of neutral AnO, which should be most abundant for An with large D[AnO], and large $D[AnO^+]$ suppresses dissociation of produced AnO^+. Unfortunately, the available IE[AnO] and $D[AnO^+]$ (Table 2) are too uncertain to interpret the observed oxide speciation in detail. The dioxide ion abundances were more disparate than for the monoxides—$UO_2^+ \gg NpO_2^+ \gg PuO_2^+ > ThO_2^+$ (not observed)—with *typical* AnO_2^+ abundances, $\{I[AnO_2^+]/I[An^+]\} \times 100$, varying from ∼20 for U to ∼0.5 for Np and ∼0.01 for Pu. That PuO_2^+ was detected only concomitant with copious Pu^+ and PuO^+ presumably reflects the large value of IE[PuO_2] (Table 2); the concentration of neutral PuO_2 was probably more substantial. Pentavalent ThO_2^+ was never detected, but tetravalent $ThO(OH)^+$ was a minor constituent.

The LA/PRD approach has the advantage of simultaneously studying the reactivities of co-ablated M^+ and MO^+. However, the presence of substantial MO^+ introduces the possibility of reactions involving O-transfer which might result in M^+-L^* products indistinguishable from those produced from naked M^+ (e.g., $M^+ + C_2H_4 \rightarrow M^+-C_2H_2 + H_2$ and $MO^+ + C_2H_4 \rightarrow M^+-C_2H_2 + H_2O$ could not be discriminated). For AnO^+ and CeO^+, the $D_0°[MO^+]$ are sufficiently large (>700 kJ mol^{-1}) to generally exclude O-transfer on thermodynamic grounds.[24] In the case of the dioxide ions, only UO_2^+ was sufficiently abundant to feasibly account for some of the observed AnO^+-L^* products; however, the large dissociation energy of $D_0°[OU^+-O] = 740$ kJ mol^{-1} [25] also generally precludes O-transfer from UO_2^+. Such might not be the case with PuO_2^+ from which O-abstraction should be more facile, but the PuO_2^+ concentration was too minuscule to account for the measured PuO^+-L^*.

Another potential complication of LA/PRD is that nascent laser-ablated ions may possess substantial translational and internal energies. The translational energies could be well estimated, and the collisional energies (KE_{CM}) were comparable for all An^+. Thus, although KE_{CM} may enable adiabatically endoergic processes, that complication was eliminated in the interpretation of the results by comparing ion reactivities under identical conditions. The degree of internal excitation is more difficult to assess but comparison of previous LA/PRD results for Ln^+,[8] An^+, and AnO^+ [17] with those obtained from longer time scale FTICR-MS experiments[5−7,15,16,19,20] indicated that observed reactivities reflect the intrinsic ground-state ion chemistry.

The notation "M^+-L^*" is intended to convey the aggregate product ion compositions without specifying charge distribution or structure. Some *plausible* structure assignments are as follows: $M^+-C_2H_4 = M^+-\eta^2$-$H_2C{=}CH_2$; $M^+-C_4H_6 = M^+-\eta^4$-$H_2C{=}CH{-}CH{=}CH_2$; and $M^+-C_6H_6 = M^+-\eta^6$-*c*−C_6H_6 (benzene). The ion, $M^+-C_8H_8$, could reasonably be assigned as $M^+-\eta^8$-*c*−C_8H_8 (cyclooctatetraene, COT) or $C_2H_2-M^+-C_6H_6$.[26] The limited dynamic range of the ion detection system and possible reactant depletion effects counsel that the most reliable reactivity comparisons were for co-ablated M^+ (or MO^+) produced at roughly comparable intensities. Comparisons of results for different targets were less accurate but proved qualitatively valid. The variable detection limits, specified by "(<)" in the tables, reflect the discrepant parent ion intensities. The results are tabulated as measured ion intensities (in mV) to allow direct comparison of absolute ion yields between experiments.

Reactions with Ethene and cis-2-Butene. All of the significant products using the primary targets specified above are included in Table 3, and representative mass spectra are shown in Figures 1 and 2. No MO^+ reaction products were detected for either linear alkene. Ethene was the least reactive substrate; the key result evident in Table 3 was that Pu^+ was

(21) Lias, S. G.; Bartmess, J. E.; Liebman, J. F.; Holmes, J. L.; Levin, R. D.; Mallard, W. G. Gas-Phase Ion and Neutral Thermochemistry. *J. Phys. Chem. Ref. Data* **1988**, *17*, Suppl. 1.

(22) Hildenbrand, D. L.; Gurvich, L. V.; Yungman, V. S. *The Chemical Thermodynamics of Actinide Elements and Compounds, Part 13, The Gaseous Actinide Ions*; I.A.E.A.: Vienna, 1985.

(23) Brewer, L.; Rosenblatt, G. M. In *Advances in High-Temperature Chemistry*; Eyring, L., Ed.; Academic Press: New York, 1969; Vol. 2, pp 1−83.

(24) Heinemann, C.; Cornehl, H. H.; Schröder, D.; Dolg, M.; Schwarz, H. *Inorg. Chem.* **1996**, *35*, 2463−2475.

(25) Armentrout, P. B.; Beauchamp, J. L. *Chem. Phys.* **1980**, *50*, 21−25.

(26) Schröder, D.; Sulzle, D.; Hrusak, J.; Böhme, D. K.; Schwarz, H. *Int. J. Mass Spectrom. Ion Processes* **1991**, *110*, 145−156.

Table 3. Product Abundances for the Reactions $M^+ + C_2H_4$ and $M^+ + C_4H_8$[a]

M^+	$+C_2H_4$		$+C_4H_8$			
	$I[M^+]$	$A[M^+-C_2H_2]$	$I[M^+]$	$A[M^+-C_4H_6]$	$A[M^+-C_4H_4]$	$A[M^+-C_2H_2]$
		U−Pu				
U^+	∼10	∼9	110	0.8	0.11	0.6
Pu^+	∼1000	(<0.05)	150	0.2	(<0.05)	(<0.05)
		Np−Pu				
Np^+	350	0.3	250	0.4	0.02	0.14
Pu^+	350	(<0.03)	260	0.1	(<0.01)	(<0.04)
		Ce−Th−(Pu)				
Ce^+	20	5	8	∼7	(<3)	∼7
Th^+	40	*b*	30	0.6	1	*b*
Pu^+	60	(<0.3)	20	0.5	(<0.1)	(<0.5)

[a] Ion intensities, $I[M^+]$, are in mV. Product abundances are $A[M^+-L^*] = \{I[M^+-L^*]/I[M^+]\}100$. Most abundances are considered accurate to within 10%, except for those otherwise specified (e.g., $A[U^+-C_2H_2] \approx 9$), which may be uncertain by up to 50% (due to inordinately large or small reactant ion intensities). Abundance values in parentheses, such as (<0.1), indicate that the product ion was not detected above the noise level; for scarce M^+ such as Ce^+, this abundance detection limit was as large as 15. [b] $A[^{232}Th^+-C_2H_2]$ could not be accurately determined because it is isobaric with $^{242}PuO^+$.

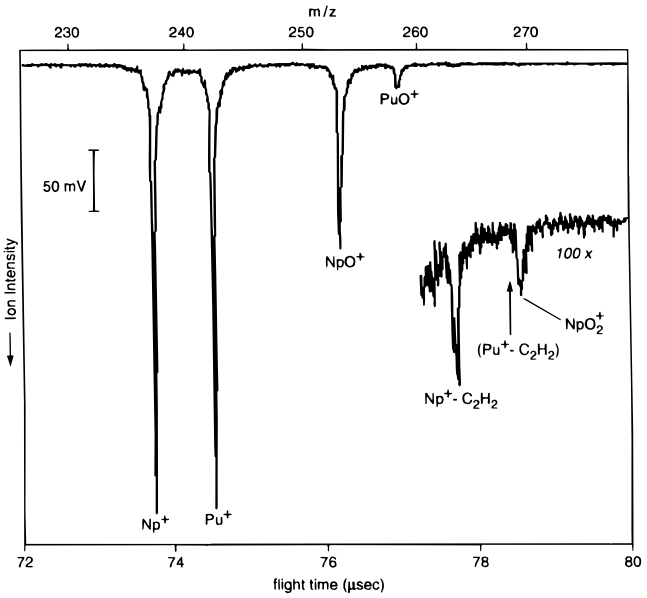

Figure 1. Mass spectrum for ablation of the **Np−Pu** target into C_2H_4.

much less reactive than U^+, Np^+, or Ce^+ (only Pu^+ was unreactive). In progressing to more reactive 2-butene, all M^+ were found to react to varying degrees, with double dehydrogenation and cracking (to acetylene) appearing as channels for the more reactive M^+: Ce^+, Th^+, U^+, and Np^+. In contrast to its inertness toward C_2H_4, Pu^+ did react with C_4H_8 though to a lesser extent than the other An^+. Pu^+ induced only single dehydrogenation to $Pu^+-C_4H_6$ with a yield smaller than for the other An^+, which additionally induced double dehydrogenation and cracking to produce $An^+-C_4H_4$ and $An^+-C_2H_2$. For Th^+ in particular, double dehydrogenation appeared as a primary reaction channel. The $Th^+-C_4H_4$ product may correspond to the bis-acetylene complex, $C_2H_2-Th^+-C_2H_2$, the formation of which could reflect a particular ability of the quasi-d-element ion, Th^+, to induce C−C activation in 2-butene.

Reactions of M^+ and MO^+ with Cyclohexene and 1,5-Cyclooctadiene. As indicated in Table 4 and illustrated for U^+/Pu^+ in Figure 3, the primary products of reaction with C_6H_{10} were $An^+-C_6H_6$ (An = Th, U, Np, and Pu), and $AnO^+-C_6H_6$ (An = Th and U). Also evident in Figure 3 is a small peak due to $U^+-C_6H_4$, presumably a benzyne complex. In contrast to the results with ethene and 2-butene, the yields of the $An^+-C_6H_6$ were comparable for all four An^+ with relatively small (<50%) differences in measured reactivities. The mass resolution was adequate to conclude that $An^+-C_6H_8$ were not produced at the detection limit (the resolution is evident in Figure 3 where a small $U^+-C_6H_4$ peak is apparent adjacent to

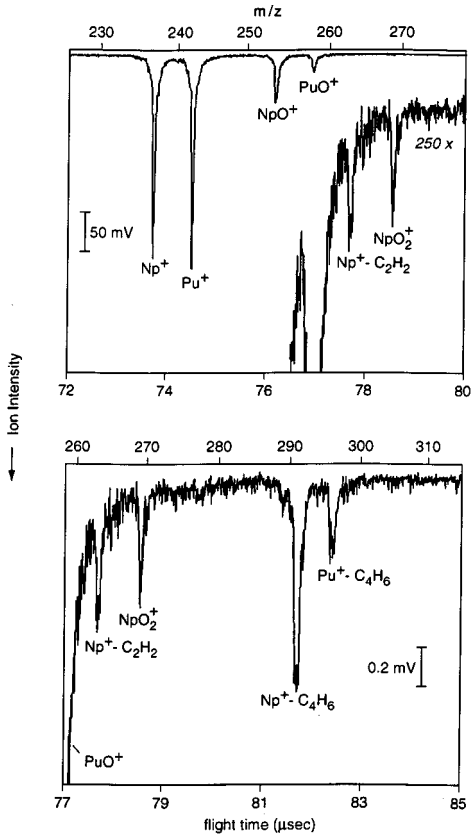

Figure 2. Mass spectrum for ablation of the **Np−Pu** target into C_4H_8.

Table 4. Product Abundances for the Reactions $M^+ + c-C_6H_{10}$ and $MO^+ + c-C_6H_{10}$[a]

M^+	$I[M^+]$	$A[M^+-C_6H_6]$	$I[MO^+]$	$A[MO^+-C_6H_6]$
		U−Pu		
U^+	220	0.6	320	0.2
Pu^+	270	0.8	100	(<0.1)
		Np−Pu		
Np^+	132	0.6	160	(<0.03)
Pu^+	400	0.9	170	(<0.03)
		Ce−Th−(Pu)		
Th^+	140	0.9	150	0.7

[a] See footnote *a* of Table 3.

Table 5. Product Abundances for the Reactions $M^+ + c\text{-}C_8H_{12}$ and $MO^+ + c\text{-}C_8H_{12}$[a]

M^+	$I[M^+]$	$A[M^+-C_8H_8]$	$A[M^+-C_6H_6]$	$I[MO^+]$	$A[MO^+-C_8H_{10}]$	$A[MO^+-C_8H_8]$
			U−Pu			
U^+	120	0.3	0.6	240	(<0.03)	0.04
Pu^+	680	0.6	0.1	80	0.2	(<0.04)
			Np−Pu[b]			
Np^+	280	0.8	0.2	100	0.15	(<0.01)
Pu^+	300	0.6	0.05	40	0.07	(<0.02)
			Ce−Th−(Pu)			
Ce^+	1.3	(<15)	(<15)	240	0.05	(<0.02)
Th^+	38	1	0.2	35	0.3	0.08
Pu^+	3	~2	(<1)	2	(<15)	(<15)

[a] See footnote *a* of Table 3. [b] In addition, $A[Np^+-C_8H_6] = 0.1$; $A[Pu^+-C_8H_6]$ (<0.05); $A[Pu^+-C_6H_8] = 0.1$; and $A[Np^+-C_6H_8]$ (<0.2). Another set of results is shown in Figure 4.

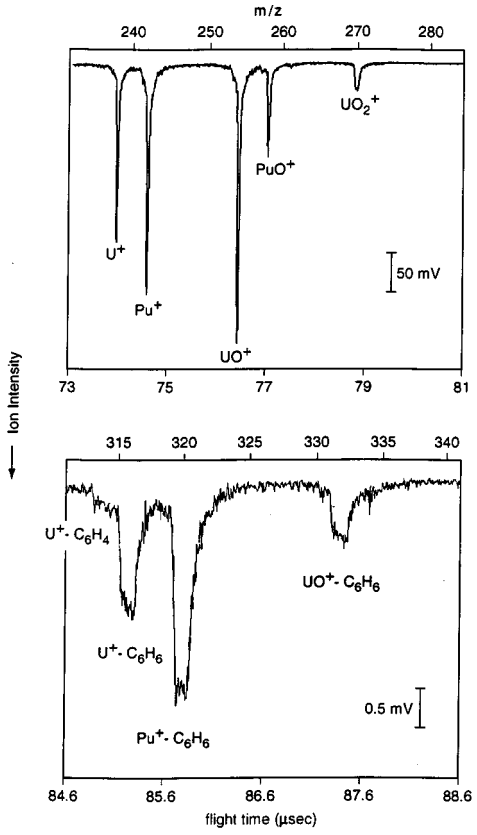

Figure 3. Mass spectrum for ablation of the **U−Pu** target into C_6H_{10}.

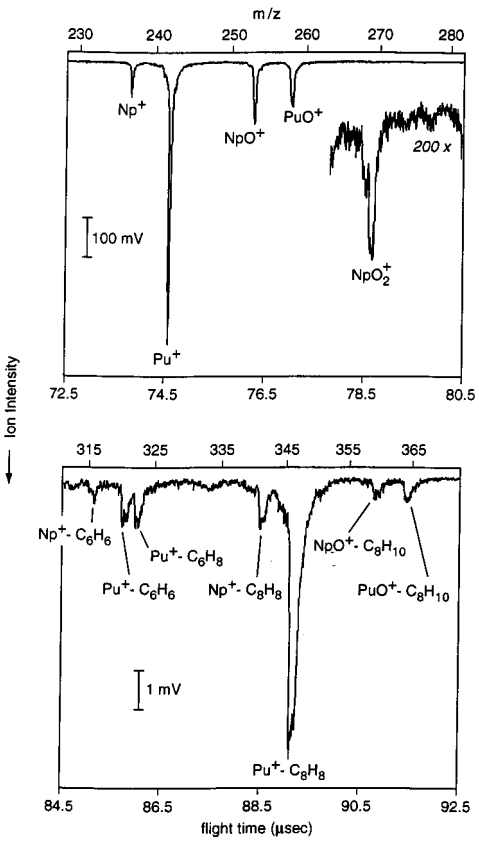

Figure 4. Mass spectrum for ablation of the **Np−Pu** target into C_8H_{12}.

the major $U^+-C_6H_6$ peak). The absence of C_6H_8 may be attributed to the exothermic loss of H_2 from cyclohexadiene to produce benzene: $C_6H_8 \rightarrow C_6H_6 + H_2 + 23$ kJ mol^{-1}. Whereas UO^+ and ThO^+ dehydrogenated cyclohexene to benzene, as found previously,[17] both NpO^+ and PuO^+ were comparatively inert.

The primary complex ions listed in Table 5 for reactions with C_8H_{12} were $An^+-C_8H_8$ (double-dehydrogenation) and $An^+-C_6H_6$ (cracking). In accord with the abundances of the $An^+-C_6H_6$ (Table 5), reactions of Th^+, U^+, and Np^+ with COD resulted in detectable amounts of $An^+-C_2H_2$—however, the greater $An^+-C_6H_6$ abundances in Table 5 are provided as the best indication of relative cracking (i.e., C−C activation) efficiencies. The abundances of these cracking and other minor products generally reflected the comparative An^+ (and AnO^+) reactivities revealed from the primary dehydrogenation product abundances. The reactant and product mass spectra for Np^+/Pu^+ + COD are shown in Figure 4. All four An^+ produced both $An^+-C_8H_8$, presumably a COT complex resulting from double H_2-elimination, and additionally induced cracking to form $An^+-C_6H_6$ (+ ethane). Whereas Th^+, U^+, Np^+, and Pu^+ were all comparably effective at doubly dehydrogenating COD to C_8H_8, Pu^+ was apparently less effective at cracking COD to yield $Pu^+-C_6H_6$. The mass resolution was adequate to exclude $An^+-C_8H_{10}$ products to the detection limit (e.g., see Figure 4 where $Pu^+-C_6H_6$ and $Pu^+-C_6H_8$ are clearly resolved). For 1,3,5-cyclooctatriene, dehydrogenation to COT is endothermic by 115 kJ mol^{-1} and dehydrogenation/cracking to $C_6H_6 + C_2H_2$ is endothermic by 146 kJ mol^{-1}.[21] That these endothermic processes evidently occurred suggests that the bonding in $An^+-C_8H_8$, presumably An^+-COT and/or C_2H_2-$An^+-C_6H_6$,[26] is substantially stronger than in undetected $An^+-C_8H_{10}$.

All four AnO^+ reacted with C_8H_{12}, but the product distributions were quite disparate. Whereas earlier LA/PRD studies failed to detect any reactivity of CeO^+ [17] some $CeO^+-C_8H_{10}$ could be detected ($A = 0.05$) in the present study due to the

larger amount of CeO^+ reactant. Co-ablated NpO^+ and PuO^+ produced roughly comparable amounts of the single H_2-loss product, $AnO^+-C_8H_{10}$ (NpO^+ may have been *slightly* more reactive). In contrast, ThO^+ additionally induced appreciable double dehydrogenation to $ThO^+-C_8H_8$, and $UO^+-C_8H_8$ was the dominant product.

Summary and Analysis of Comparative Reactivities. The results discussed above, detailed in Tables 3−5 and illustrated in Figures 1−4, are summarized here. The present results for Ce^+, Th^+, and U^+ are essentially consistent with previous observation of comparable reactivities for these naked M^+. The inert character of CeO^+ compared with reactive ThO^+ and UO^+ [17] was again manifested in the present work. The key new results are the comparative reactivities of An^+ and AnO^+ for An = U, Np, and Pu which are summarized below by comparing the relative abundances for the primary reaction products. In the summary, "≈" indicates similar abundances to within a factor of 2, ">" indicates a difference in the range of 2× to 10×, and "≫" indicates a difference greater than 1 order of magnitude; parentheses (e.g., "(≫Pu^+)") designate products which were not detected.

(1) $An^+ + C_2H_4 \rightarrow An^+\text{-}C_2H_2 + H_2$ U^+ (>> Pu^+) Np^+ (>> Pu^+)

(2) $An^+ + C_4H_8 \rightarrow An^+\text{-}C_4H_6 + H_2$ $U^+ \approx Np^+ > Pu^+$

(3) $An^+ + C_4H_8 \rightarrow An^+\text{-}C_4H_4 + 2H_2$ U^+ (> Pu^+) Np^+ (> Pu^+)

(4) $An^+ + C_4H_8 \rightarrow An^+\text{-}C_2H_2 + C_2H_6$ U^+ (>> Pu^+) Np^+ (> Pu^+)

(5) $An^+ + C_6H_{10} \rightarrow An^+\text{-}C_6H_6 + 2H_2$ $U^+ \approx Np^+ \approx Pu^+$

(6) $An^+ + C_8H_{12} \rightarrow An^+\text{-}C_8H_8 + 2H_2$ $U^+ \approx Np^+ \approx Pu^+$

(7) $An^+ + C_8H_{12} \rightarrow An^+\text{-}C_6H_6 + C_2H_6$ $U^+ \approx Np^+ > Pu^+$

(8) $AnO^+ + C_6H_{10} \rightarrow AnO^+\text{-}C_6H_6 + 2H_2$ UO^+ (> NpO^+ / PuO^+)

(9) $AnO^+ + C_8H_{12} \rightarrow AnO^+\text{-}C_8H_{10} + H_2$ (UO^+ <) $NpO^+ \approx PuO^+$

(10) $AnO^+ + C_8H_{12} \rightarrow AnO^+\text{-}C_8H_8 + 2H_2$ UO^+ (> NpO^+ / PuO^+)

Scandium is a quasi-f-block element, and the available BDE-[Sc^+-L] values[27] suggest that the observed reactions are thermodynamically plausibile. For some reactions (e.g., formation of $An^+-C_6H_6$ (+ ethane) from COD), the energy deposited (e.g., >200 kJ mol^{-1}) in the nascent complex ion might result in metastability toward fragmentation on a time scale longer than the ∼100 μs within which products were detected by LA/PRD; it was not possible in the present experiments to discern fragmentation in the flight tube from peak shapes or splittings. Quite different product abundances and compositions might be observed using techniques such as FTICR which can be carried out under conditions involving multiple sequential ion−molecule collisions.

By comparing the yields of U^+-L^* and Np^+-L^* relative to Pu^+-L^* it was possible to indirectly establish that U^+ and Np^+ are comparably effective at both C−H and C−C activation for the alkene substrates employed here. This result is consistent with the conventional oxidative insertion mechanism which requires two unpaired non-f valence electrons for participation in σ-bonding in the H−An^+−C or C−An^+−C activated complex because both U^+ and Np^+ exhibit ground or very low-lying configurations with two such electrons (Table 1). Whereas the U^+ versus Np^+ comparison does not reveal the possibility of 5f participation in hydrocarbon activation, the results for Pu^+ do illuminate the role of 5f electrons. With both ethene and 2-butene, it was found that the dehydrogenation (and cracking for butene) capability of Pu^+ was distinctly less than that of U^+ or Np^+. These results are taken to reflect the ∼100 kJ mol^{-1} necessary to excite ground Pu^+ to a configuration with two unpaired non-5f valence electrons (Table 1) and demonstrate that the 5f electrons of ground Pu^+ are not effective at C−H or C−C activation for these linear alkenes.

The situation for cyclic C_6H_{10} and C_8H_{12} appears entirely different from that with ethene and 2-butene in that U^+, Np^+, and Pu^+ all induce double dehydrogenation of these cyclic substrates with roughly comparable efficiencies. The greater reactivity of the cyclic alkenes can be rationalized on both thermodynamic and mechanistic grounds. With regard to thermochemical considerations, the formation of benzene from cyclohexene requires only 88 kJ mol^{-1} [21] and the $An^+-C_6H_6$ bond energy is undoubtedly substantially greater than this quantity.[27] Dehydrogenation of COD to COT requires 239 kJ mol^{-1}. In the condensed phase, the U−COT bond is quite strong with BDE[U−COT] = 347 kJ mol^{-1} (average for $U(COT)_2$).[12] Estimating gas-phase M^+-L bond energies from such condensed-phase thermochemistry is a crude approach but it might be presumed that the BDEs for U^+-COT and transuranium An^+-COT exceed the 239 kJ mol^{-1} required to produce COT from COD. On mechanistic grounds, the cyclic hydrocarbons possess 2′ allylic C−H bonds which should cleave relatively easily to produce the C−An^+−H activated intermediate; specifically, the 2′ allylic C−H bonds in cyclohexene and COD should be appreciably more susceptible to fragmentation than the terminal C−H bonds in 2-butene. For comparison, the H−{C_6H_9} bond strength is ∼14 kJ mol^{-1} smaller for the 2′ allylic C−H bond of cyclohexene than for the 1′ terminal C−H bond of 2-pentene.[21] Invoking a "curve-crossing" mechanism for M^+ excitation to a "divalent" state in the course of insertion into a C−H bond,[7] the activation barrier should be lowered by weakening of the C−H bond and all insertion processes should become more efficient. An exponential dependence on the activation energy would particularly enhance insertion for those M^+ with larger barriers (i.e., greater excitation energies to a "divalent" configuration). An additional effect which could generally enhance activation of the cyclic alkenes is their greater polarizabilities—as suggested by lower ionization energies[21]—which would stabilize transitory M^+-L adducts prior to oxidative insertion. An additional mechanistic consideration is the presumably greater facility of β-H abstraction from the adjacent C−H site in the cyclic alkenes; in contrast, for 2-butene a 1,4-H_2 elimination must be achieved.

Although Pu^+ was approximately as effective as U^+ and Np^+ at dehydrogenation of COD (e.g., $A[U^+-C_8H_8] = 0.3$ vs $A[Pu^+-C_8H_8] = 0.6$), cracking to produce $An^+-C_6H_6$ was significantly more facile for U^+ and Np^+ compared with Pu^+. Because cracking of COD to benzene and ethane is intrinsically *exothermic* by −60 kJ mol^{-1},[21] a thermodynamic rationalization would appear inappropriate, and it is surmised that Pu^+ is less effective at C−C activation, in coincidence with its greater promotion energy to a non-f "divalent" state and a relative inefficiency of the 5f electrons at participation in C−Pu^+-C σ-bonding. The target C−C bonds for elimination of ethane from COD are probably somewhat stronger than the allylic C−H bond at which dehydrogenation is initiated: considering 1-butene for reference, the allylic C−H bond is ∼30 kJ mol^{-1} weaker than the C(2)−C(3) bond.[21] In summary, the present results do not exclude the possibility for 5f participation in the π-bonding in the An^+-L^* complexes and may admit a minor

(27) Freiser, B. S., Ed.; *Organometallic Ion Chemistry*; Kluwer: Dordrecht, The Netherlands, 1996.

role for 5f-electrons in C−H/C−C activation but the results with ethene and 2-butene clearly indicate that it is necessary to excite Pu^+ to a prepared "divalent" configuration with two non-5f electrons to achieve efficient C−H activation, presumably by oxidative insertion, and that the 5f-electrons are accordingly ineffective at σ-bonding in C−Pu^+−H activated complexes. Cracking via C−C activation by Pu^+ appeared even more restricted compared with the other An^+. It should be emphasized that significant diminishment in 5f bonding might be anticipated in proceeding from U^+ to Np^+ to Pu^+ due to both energetic stabilization of the 5f electrons and spatial contraction of the 5f orbitals,[18] and also that the 5f-bonding effectiveness may differ in C−An^+−H versus C−An^+−C bonding. The apparently limited ability of Pu^+ to activate C−C bonds in particular is reminiscent of the behavior of the early-d-block transition metals and lanthanides[28] and illustrates the increasing tendency toward lanthanide-like behavior upon proceeding across the actinide series.

As with Ce^+ and Th^+,[17,20] the addition of an oxo ligand to the metal center of the An^+ studied here dramatically affected their reactivities. According to a model proposed by Cornehl et al. to explain disparate LnO^+ reactivities,[19] a high IE[LnO] and a low IE[L] are favorable to LnO^+−L electrostatic interaction and subsequent activation via a multicentered activation complex. In their work with ThO^+ and UO^+, Cornehl et al.[20] suggested a similar mechanism for efficient dehydrogenation of 1,4-cyclohexadiene by ThO^+, due to the relatively available (6d) electron associated with Th; they furthermore proposed bonding participation of the 5f electrons of UO^+ in explaining its appreciable dehydrogenation activity. The approximate IE[AnO] values given in Table 2 predict that ThO^+ should be more reactive via a multicentered complex compared with UO^+, NpO^+, and PuO^+, which latter three AnO^+ should be comparably effective at activation through electrostatic AnO^+−L interactions according to their similar IE[AnO]. The IE[L] for 1,4-cyclohexadiene and the organic substrates used here are as follows[21] (in kJ mol^{-1}; accurate to $\leq$2 kJ mol^{-1}): IE[1,4-*c*−C_6H_8] = 851, IE[C_2H_4] = 1014, IE[*cis*-2-C_4H_8] = 879, and IE[*c*−C_6H_{10}] = 863 (IE[COD] is estimated as ∼860). On the basis of the IE correlation and the apparent affinity of ThO^+ and UO^+ for 1,4-*c*−C_6H_8, similar affinities would be expected for UO^+, NpO^+, and PuO^+ with *c*−C_6H_{10} and COD. However, from reaction 8 above, it is evident that only UO^+ among these three AnO^+ species activated *c*−C_6H_{10}. This distinctive behavior suggests a specific role for the higher-energy and more extended 5f electrons at the metal center of UO^+. From reactions 9 and 10, it is seen that whereas all three AnO^+ species activated COD, UO^+ induced double dehydrogenation (to UO^+−C_8H_8) while NpO^+ and PuO^+ formed only the single H_2 loss product, AnO^+−C_8H_{10}. This discrepancy again indicates unique behavior of UO^+, consistent with 5f electron participation there. In accord with the above-noted diminishment in 5f bonding upon proceeding from U to Pu, it would appear that the 5f orbitals of UO^+ may be appreciably more effective at C−H activation than those of either NpO^+ or PuO^+. In the case of COD dehydrogenation, activation/H_2 loss with NpO^+ and PuO^+ (and possibly UO^+) may occur by a multicentered intermediate, such as in Scheme 2. Specifically, for the OU^+−C_8H_{10} complex, dehydrogenation is presumed to involve the relatively chemically active 5f orbitals at the U-center, possibly via a conventional oxidative insertion mechanism into a C−H bond. Although CeO^+ was minimally reactive, its behavior was qualitatively similar to that of NpO^+ and PuO^+ (i.e., single dehydrogenation of COD albeit at a lower efficiency), suggesting noninvolvement of the f electrons for all three of these MO^+. As noted previously,[20] ThO^+ should perhaps be considered as a quasi-d-block MO^+, with a more loosely bound radical valence electron than its heavier AnO^+ congeners; this characteristic may be reflected in its relatively high dehydrogenation activity.

Scheme 2

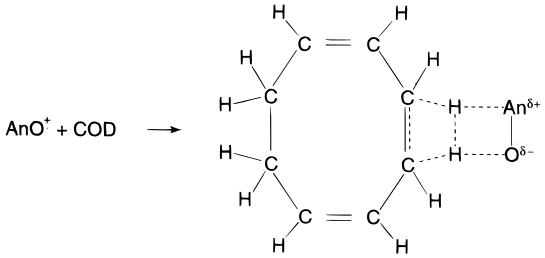

Conclusions

Gas-phase reactions of An^+ and AnO^+ (An = Th, U, Np, Pu) with alkenes of varying degrees of susceptibility to activation of C−H bonds (dehydrogenation) and C−C bonds (cracking) were investigated and compared with those for Ln^+ and CeO^+. As Pu^+ is the first An^+ to require a substantial excitation energy (∼100 kJ mol^{-1}) to promote a 5f electron to a more extended valence orbital (6d/7s), the comparative reactivities of U^+, Np^+, and Pu^+ elucidated the role of 5f electrons in direct participation in C−H activation by oxidative insertion. The significantly lesser reactivity of Pu^+ with ethene and 2-butene confirmed Ln^+-like behavior and noninvolvement of the 5f electrons of Pu^+. A smaller distinction between the reactivities of Pu^+ and the preceding An^+ with regard to cycloalkene dehydrogenation may be attributed to the greater polarizabilities and relatively weak allylic C−H bonds available for attack in those substrates. That Pu^+ was apparently nearly as effective as Np^+ at dehydrogenating these cyclic alkenes contrasts with the discrepant behaviors of comparable Ln^+ under similar conditions and may reflect 5f−6d hybridization, as has been suggested for An^{IV}−$(COT)_2$ compounds.[29] The distinctively lesser reactivity of Pu^+ again appears in elimination of ethene from COD, presumably reflecting a stronger C−C bond to activate which heightens the energy barrier to the activated C−An^+−C complex and accentuates the greater energy to excite Pu^+ to a prepared "divalent" state compared with the preceding An^+; Pu^+ is apparently rather Ln^+-like in its particularly reduced capability to activate C−C bonds.

As had been established previously for the lanthanides,[19] the addition of an oxo ligand to the naked metal ions dramatically affected reactivities. In particular, UO^+ (like ThO^+) was found to double dehydrogenate cyclohexene and COD, while NpO^+ and PuO^+ (like CeO^+) were apparently inert toward cyclohexene and only singly dehydrogenated COD. Assuming a model involving a multicentered activation complex of the cyclic alkenes with facial coordination of an allylic H−C(3) and adjacent H−C(4) by $M^{\delta+}$−$O^{\delta-}$ (Scheme 2), the relatively high activity of ThO^+ can be attributed to the large IE[ThO];[19,20] the smaller activities of the other MO^+ (especially CeO^+) correspond to their smaller IEs (Table 2 and IE[CeO] = 473(10) kJ mol^{-1}).[21] Within this picture the relatively high reactivity of UO^+ is evidently anomalous since IE[UO] ≈

(28) Weisshaar, J. C. *Acc. Chem. Res.* **1993**, *26*, 213-219.

(29) Karraker, D. G.; Stone, J. A.; Jones, E. R., Jr.; Edelstein, N. *J. Am. Chem. Soc.* **1970**, *92*, 4841−4845.

IE[NpO] ≈ IE[PuO]. A more refined picture of the affinity of the MO^+ for the π-bonded substrate should consider polarizability (rather than vertical electron transfer) and the role of the valence shell electrons at the metal center. In the case of UO^+ in particular, it has been postulated that the 5f electrons at the metal center play a central role in C−H activation.[20] The electronic structure of UO^+ is uncertain,[30] but the energy separation between the 5f and 6d orbitals of uranium should be smaller than for a corresponding Np or Pu center[18] and 5f−6d hybridization such as supposedly occurs in σ-bonded $U-(CH_3)_3$[31] may be feasible in UO^+. The 5f−6d-hybridized electrons of UO^+ could more effectively participate in σ-bonding in a $C-U(O)^+-H$ oxidative insertion intermediate. Both NpO^+ and PuO^+ appear to behave rather similarly to LnO^+; a transition from bonding (or d/f hybridized) 5f electrons in UO^+ to essentially localized 5f electrons in NpO^+ could account for the observed chemistries.

Acknowledgment. This work was sponsored by the Division of Chemical Sciences, Office of Basic Energy Sciences, U.S. Department of Energy, under Contract DE-AC0596OR22464 at Oak Ridge National Laboratory with Lockheed Martin Energy Research Corp. The author is grateful to Professor H. Schwarz for providing preprints of refs 19 and 20.

JA973182E

(30) Krauss, M.; Stevens, W. J. *Chem. Phys. Lett.* **1983**, *99*, 417−421.
(31) Ortiz, J. V.; Hay, P. J.; Martin, R. L. *J. Am. Chem. Soc.* **1992**, *114*, 2736−2737.